Applied Surface Science 375 (2016) 50–56

Contents lists available at ScienceDirect

Applied Surface Science

journal homepage: www.elsevier.com/locate/apsusc

# Investigation of stabilization mechanism and size controlling of $Fe_3O_4$ nanoparticles using anionic chelating agents

Mohammad Reza Ghazanfari [a], Mehrdad Kashefi [a,*], Mahmoud Reza Jaafari [b]

[a] Department of Materials Science and Engineering, Ferdowsi University of Mashhad, 9177948974 Mashhad, Iran
[b] Biotechnology Research Center, Nanotechnology Research Center, School of Pharmacy, Mashhad University of Medical Sciences, Mashhad, Iran

ARTICLE INFO

*Article history:*
Received 8 December 2015
Received in revised form 15 February 2016
Accepted 7 March 2016
Available online 9 March 2016

*Keywords:*
Colloid
Iron oxide nanoparticles
Stability
Particle size
Chemical preparation
Magnetic properties

ABSTRACT

Chelating agents have potential effects on different properties of nanoparticles. $Fe_3O_4$ nanoparticles were synthesizes Using coprecipitation technique and oxalic, citric, stearic and lauric acids with concentrations of 0.5, 1, 2, and 5 vol% were utilized as the chelating agents. Subsequently, stability, structural, and magnetic properties of the samples were studied using measurement of zeta potential as well as FT-IR, XRD, DLS, TEM, and VSM analyses. It was found that the lower end of the size range was achieved for all samples utilizing 2 vol% chelating agents. So, in the present study, it was chosen as the optimum volume percentage of the chelating agents. Furthermore, for the nanoparticles treated with oxalic and citric acids, particle sizes were lower and the zeta potentials were larger comparing to those treated with stearic and lauric acids, which is an indication of their higher stabilization ability. Finally, the type of chelating agents had negligible effects on the structural and magnetic properties of the synthesized nanoparticles.



## 1. Introduction

In the past decades, developing concepts of nano-sciences and nanotechnology, the utilizations of nanomaterials are outreached in many applications such as the electronic and microelectronic technologies, gas and oil industries, renewable energy, aerospace, agriculture, and various biomedical applications [1–5]. In some applications, the nanoparticles have to be used in colloidal systems. Ferrofluid is a technical term for colloids consisting of stable distribution of magnetic nanoparticles in liquid phase [5–8].

The magnetic iron oxide nanoparticles ($\gamma$-$Fe_2O_3$ and especially $Fe_3O_4$) have been used in many in-vitro and in-vivo biomedical applications like cells detection and separation, contrast agents in magnetic resonance imaging (MRI), magnetic hyperthermia, and magnetic targeted drug delivery due to their considerable magnetic and biocompatibility properties [9–12]. As a result, the stabilization process is one of the most important steps in synthesizing the nanoparticles [10–16]. In many biomedical applications (especially in-vivo ones), in order to stabilize the nanoparticles cationic or anionic electrostatic stabilization agents are used because of their ability to create biocompatible particles with relatively small size as well as narrow size distribution compared to the steric agents [17–22].

In biomedical applications of magnetic nanoparticles, proper selection and utilization of stabilizing agents could lead to achieving optimized superparamagnetic behavior, increasing half-life time of colloids and improving the overall stability of the ferrofluid [22–24]. Many stabilizing agents such as different groups of acids not only improve electrostatic stabilization but they could also be utilized as chelating agents [23–25]. These agents could positively affect nucleation and growth by formation of protective layer on the nanoparticles surfaces [21–26]. As a result, the utilization of chelating agents could stabilize the synthesized nanoparticles and control their final size, simultaneously. So, the study of effects and mechanism of different chelating agents can lead to improve quality and properties of the synthesized nanoparticles. The chelating agents are, normally, selected based on the several factors including application, size and type of particles as well as condition of other required agents such as drugs for medicine applications. [25–29].

The present research is focused on effects of chelating agents on the stabilization process of $Fe_3O_4$ nanoparticles and also the study of size controlling mechanism the agents. In order to achieve these aims, several anionic stabilizing agents such as oxalic, lauric, citric, and stearic acids are used for stabilizing and size controlling of the nanoparticles the various effects on their structural, microstructural, and magnetic properties are also evaluated.

* Corresponding author.
*E-mail address:* m-kashefi@um.ac.ir (M. Kashefi).

http://dx.doi.org/10.1016/j.apsusc.2016.03.067
0169-4332/

## 2. Materials and methods

### 2.1. Materials

$FeCl_2{\cdot}4H_2O$ and $FeCl_3{\cdot}6H_2O$ (>99%, Merck), $NH_4OH$ (Merck) and Citric acid (>99.5%, Merck) were selected as the initial salts, the reduction agent and dispersant agent, respectively. Oxalic acid (>99.5%, Merck), lauric acid (>98%, Sigma-Aldrich), stearic acid (>98.5%, Sigma-Aldrich) and citric acid (>99.5%, Merck) were utilized as anionic chelating agents.

### 2.2. Synthesis and stabilization processes of $Fe_3O_4$ nanoparticles

Coprecipitation technique was usedto synthesize the $Fe_3O_4$ nanoparticles. The initial materials consisting of $FeCl_2{\cdot}4H_2O$ and $FeCl_3{\cdot}6H_2O$ were solved in 100 ml of deionized water according to designed stoichiometric ratio in each experimental run. To prevent oxidation of $Fe^{2+}$, the synthesis reaction was done at $N_2$ protective atmosphere. Then, $NH_4OH$ was added to the reaction solution as the reduction agent. pH and temperature were fixed for all tests at 11.5 and 90C, respectively. Facilitating homogenization, the solution was mixed by mechanical stirrer with the speed of 3000 rpm for 1 h. In orderto study the effects of chelating agents, the selected amounts (0.5, 1, 2, and 5 vol%) of each 1 M chelating agent stock were added to the independent sample solutions and were aged for 1 h while stirring with the speed of 3000 rpm. Finally, the synthesized nanoparticles were separated by the magnetic separation, centrifuged and washed by deionized water and ethanol for five times, and dried by freeze dryer.

### 2.3. Characterization

The effect of applying chelating agents on the stability properties the nanoparticles were studied by zeta potential measurement and Fourier transform infrared using Zeta meter (MALVERN, UK) and FT-IR spectrophotometer (Perkin Elmer, Walthman, USA), respectively. FT-IR spectra were recorded over the range of 400–4000 cm-1. Furthermore, the studies of microstructural properties of particles such as particles size, morphology, and size distribution were carried out by dynamic light scattering (DLS, MALVERN, UK) and transmission electron microscope (TEM, JEOL2010, Japan) techniques. Moreover, the structural properties of stabilized nanoparticles were evaluated based on the X-ray diffraction (XRD) method by X-ray diffractometer (XRD, Bruker Advance 2, Germany) using a $CuK\alpha_{1,2}$ radiation set (at 40 kV and 40 mA at room temperature with a $2\Theta$ range of 20–80° with step size and rate of 0.03° and 6 seconds, respectively). The phase identification of the samples was done by utilization of MATCH software. Finally, the M-H curves were plotted by the vibrating sample magnetometer (VSM, Meghnatis Daghigh Kavir Co., Iran).

## 3. Results and discussion

Initially, in order to investigate the influence of different concentrations of chelating agents and achieving the optimum amount, their effect on the particles size were studied. Fig. 1 shows the variations of average particles hydrodynamic size (measured by DLS technique) as a function of different concentrations of used chelating agents. As can be seen, in all samples, the particles size is decreased by increasing the agent concentration up to 2 vol% and then it is augmented. In the other word, that the minimum particles size is detected in the samples treated with 2 vol% chelating agent. The larger particle sizes at concentrations less than 2 vol% can be related to two main reasons. First one is the incomplete coating of particles surfaces due to very low concentration of agents, so the nanoparticle growth is continued and relatively larger final particle size is achieved [30]. The other reason is the agglomeration of particles owing to incomplete surface coating by agents and imperfect stabilization process. This, in turn, resulted in larger particle size measurement by the DLS technique [30–32]. Furthermore, the coated samples with chelating agent more than 2 vol% show partial increasing of particles size that is caused by the formation of relatively thick layer of the chelating agents on the particles surfaces and subsequent augmentation of their size [32,33]. In addition, these variations are more highlighted using agents with larger molecular structures like stearic acid [30–33].

Accordingly, the 2 vol% is selected as the optimum concentration to carry out other analyses such as effects of chelating agents on the stability, structural, microstructural, and magnetic properties of the nanoparticles.

### 3.1. Stability properties

Fig. 2 shows the variations of average amounts of zeta potential and zeta deviations as functions of different kinds of chelating agents at fixed concentration (2 vol%). Based on Fig. 2(a), it is evident that the zeta potential amounts for citric acid and especially oxalic acid are significantly higher than those related to stearic and lauric acids which could be an indication for higher stability of citric and oxalic acid treated colloids compared to stearic and lauric ones [32]. In fact, although the stearic and lauric acids agents have larger chains that could lead to steric stabilization, the citric and oxalic acid agents promote a stronger electrostatic stabilization (in constant time and concentration) due to their higher acidic strength and reactivity [30–34]. The high amounts (on the negative direction) zeta potential of oxalic and citric agents are created by greater number of hydroxyl groups of these agents compared to lauric and stearic acids. In fact, in negative electrostatic stabilization, the hydroxyl groups play key roles while the hydroxyl groups of citric, oxalic, lauric, and stearic acids are equal to 4, 2, 1, and 1, respectively. Besides, Fig. 2(b) represents a lower zeta deviation for samples treated with citric and oxalic acids that indicates more homogeny of stabilization process in these samples. These behaviors could be as the result of more degradability and reactivity of citric and oxalic acids compared to lauric and stearic acids [35–37].

Fig. 3 shows the FT-IR spectra of samples with and without different chelating agents. It can be seen that the sample without any chelating agent (spectrum a) shows the absorption peaks at 555 and 1590 $cm^{-1}$ which can be related to the Fe—O vibration of $Fe_3O_4$ structure [36]. Although these peaks are visible in spectra of all samples, their intensities are decreased in samples treated with chelating agents. In spectra of stearic acid and lauric acid samples (spectrum b and e) two absorption peaks are also observed at about 2924 and 2854 $cm^{-1}$ which are corresponded to the asymmetric $CH_2$ stretching and symmetric $CH_2$ stretching, respectively [38–40]. In addition, considering the presence of $Fe_3O_4$ phase in addition to the chelating agents, one can expect the partial shifts of the peaks compared to the standard ones of pure agents [41]. The other reason for these shifts could be the presence of mono-layers of hydrocarbons chains on the nanoparticles surfaces as the closed-packed crystalline structures [38–41]. In the samples treated with citric and lauric acid (spectrum c and e) the sharp peaks are observed at about 1680 and especially 1710 $cm^{-1}$ which could be the result of overlapping of absorption bands of carboxyl structures and the double bonds of utilized chelating agents [36]. While, the absorption peaks at about 1440 and 1500 $cm^{-1}$ could be a reprehensive of double bond formation which is an indication of interaction type between agent groups and nanoparticles surfaces based on the intensity of the peaks [41]. Subsequently, considering that their difference is less than 100 $cm^{-1}$, the interaction of agents and nanoparticle surfaces has the bidentate complex structure (chelating mode) between oxygen atoms of carboxyl groups

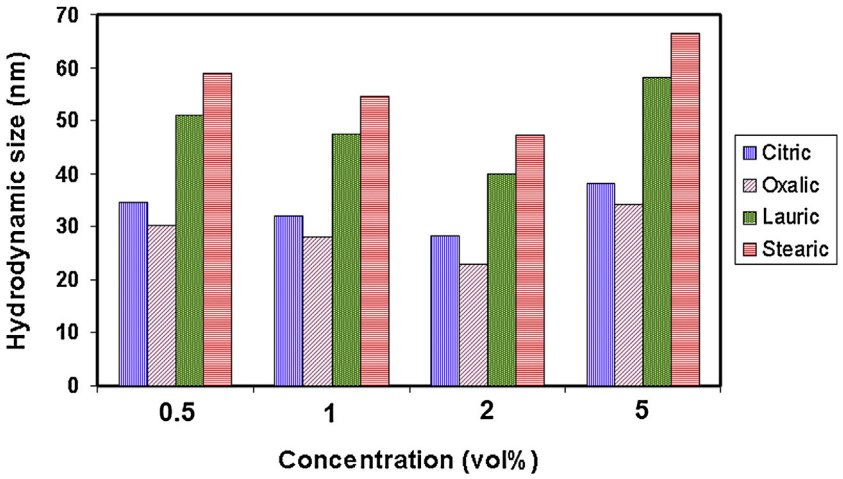


**Fig. 1.** The variations of average particles hydrodynamic size (measured by DLS technique) as a function of different concentrations of used chelating agents.

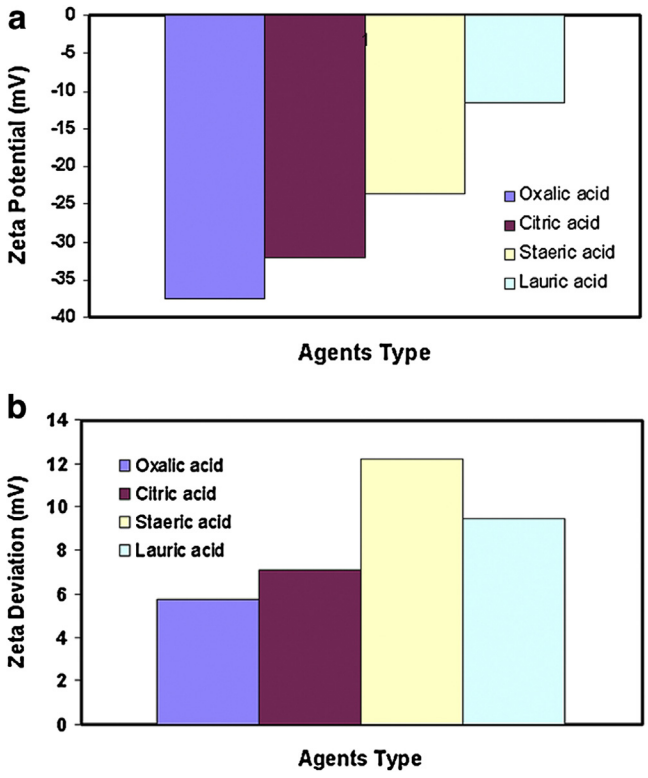


**Fig. 2.** The variations of average amounts of zeta potential and zeta deviations as functions of different kinds of chelating agents with fixed concentration (2 vol%).

and iron atoms of nanoparticles surfaces [42]. This structure can show the effective interaction between used chelating agents and surfaces of nanoparticles.

### 3.2. Microstructural properties and size controlling

Figs. 4 and 5 illustrate the variation of particles size (based on DLS analyses) as a function of different chelating agents, respectively. As can be seen, not only the particles size of citric and oxalic acid treated samples are lower than stearic and lauric acid ones, but their corresponding size distribution is also considerably narrower. The main reason is higher reactivity of citric and oxalic acids which promote particles size controlling by rapidly creation of bonding combined with electrostatic stability [42]. In addition, the carbon chains of these agents are relatively short while the lauric and especially stearic acid (as a semi-fatty acid) have large chains which can lead to slightly increase in the particles size [42].

Fig. 6 indicates the TEM micrographs of synthesized particles in presence of different chelating agents. It is clear that these micrographs are conformed with DLS results, so that the samples of oxalic acid, citric acid, lauric acid, and stearic acid show the increasing trend of particles size, respectively. Based on TEM results, the particles of oxalic acid, citric acid, lauric acid, and stearic acid is equal to 11.2, 14, 16.6, and 19.1 nm, respectively. Moreover, the morphology studies show that in all samples the particles have semi-spherical shape with appropriate shape uniformity.

### 3.3. Structural and magnetic properties

Fig. 7 illustrates the XRD diffraction patterns of different samples. In all patterns, the peaks of $Fe_3O_4$ phase are clearly observed

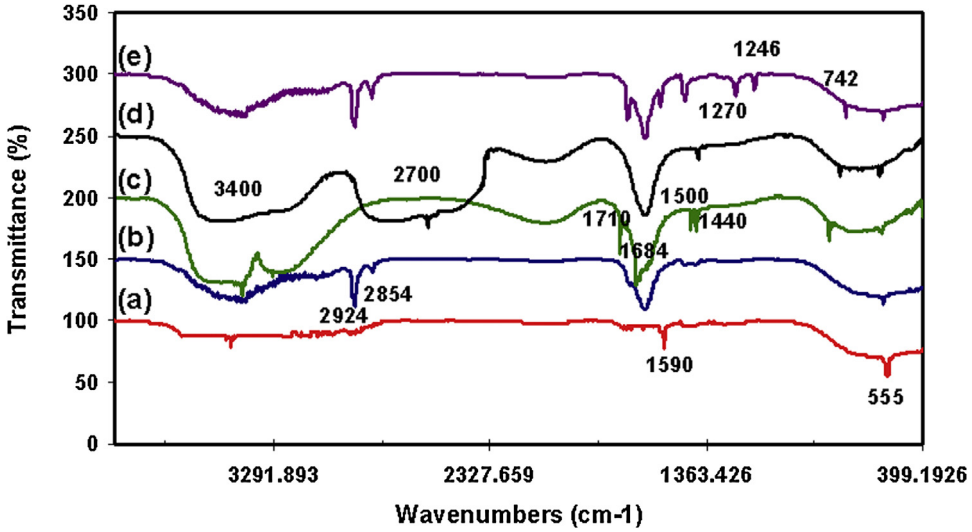


**Fig. 3.** The FT-IR spectra of samples with and without different chelating agents (Notations: (a) Pure $Fe_3O_4$, (b) Stearic sample, (c) Citric sample, (d) Oxalic sample, and (e) Lauric sample).

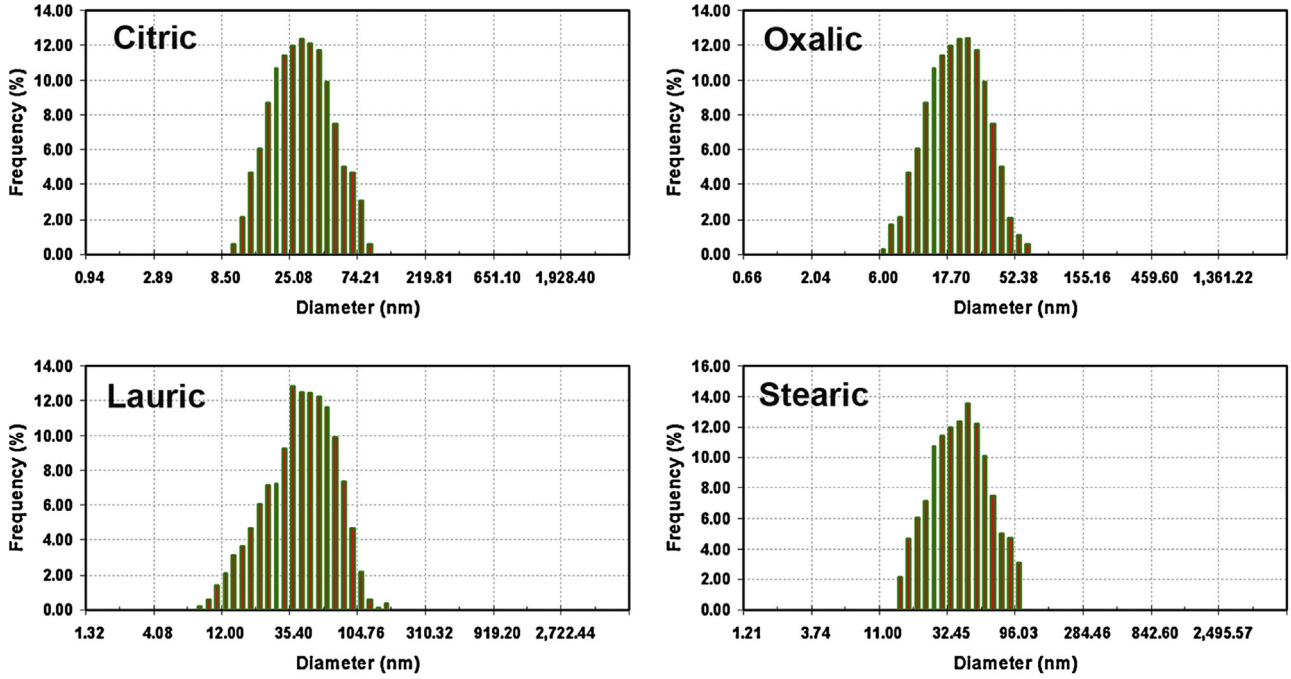


**Fig. 4.** The variations of particles size (based on DLS analyses) as functions of different chelating agents.

while no peaks of other possible undesirable phases (like goethite) can be observed. So it can be concluded that the impurities and/or undesirable phases are completely absent in the presence of the chelating agents which indicates the appropriate procedure has been applied. The peaks for original nanoparticles (without any chelating agent) are sharper owing to the larger particles size and higher crystallinity degree of the nanoparticles (about 86%) [42]. Although the particles sizes for citric and oxalic acid samples are lower comparing the ones for lauric and stearic acid samples, their peaks sharpness is also superior as a result of higher crystallinity degree and shorter chains of citric and oxalic agents [40–42]. The crystallinity degree of samples treated with oxalic, citric, stearic, and lauric acids are equal to 83%, 82%, 80%, and 79%, respectively. Although the crystallinity degrees are very close together, the nuances could cause meaningful differences in their peaks broadening [38–42]. As a result, it can be concluded that the utilization of different types of chelating agents has negligibly effects on the structural properties of synthesized nanoparticles, and, all samples have equal structural properties.

Fig. 8 shows the variation of magnetization amounts as a function of applied magnetic field for different samples (M-H curve). The amount of saturation magnetization ($M_s$) of sample without any chelating agent (curve a) is the highest (about 64 emu/g) as a result of larger size of magnetic particles [42]. The M-H curves of samples treated with different chelating agents show fairly similar amounts of $M_s$ (in the range of 53–59 emu/g), indicating comparable magnetic properties. The small differences in their magnetic properties can be as a result of the variation in the crystallinity degree and particles size [37–42].

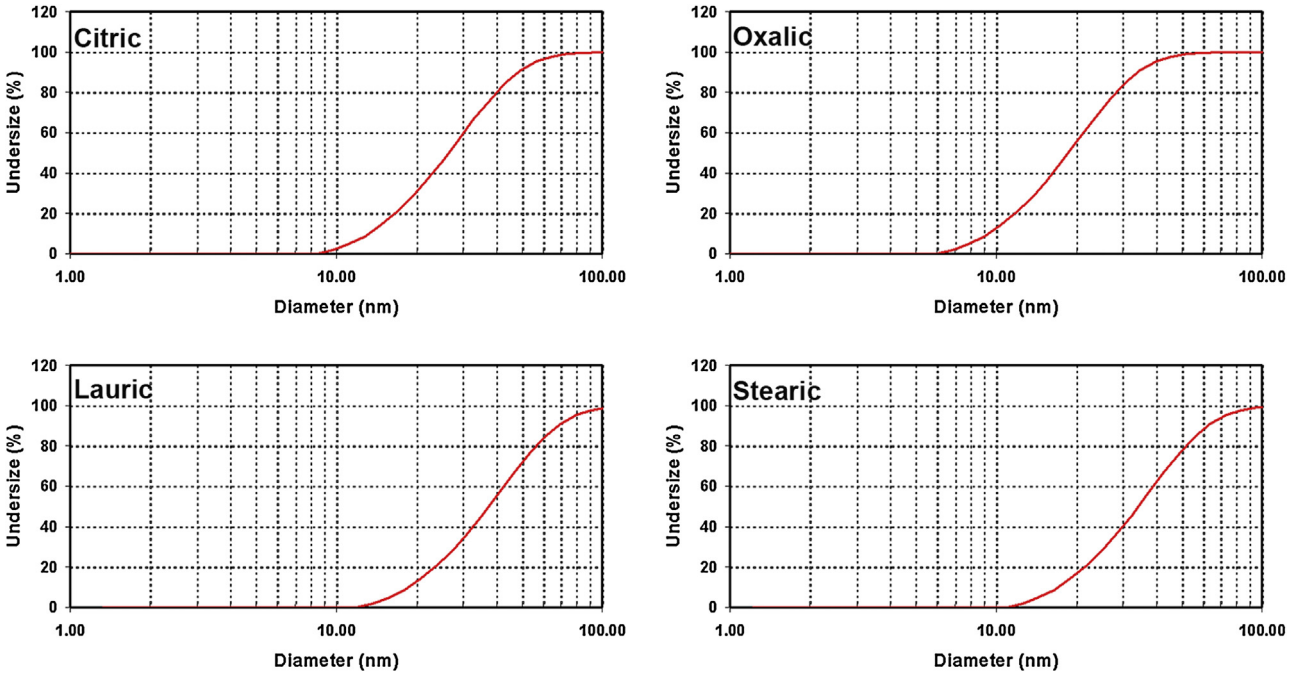


**Fig. 5.** The variations of particles undersize limits (based on DLS analyses) as functions of different chelating agents.

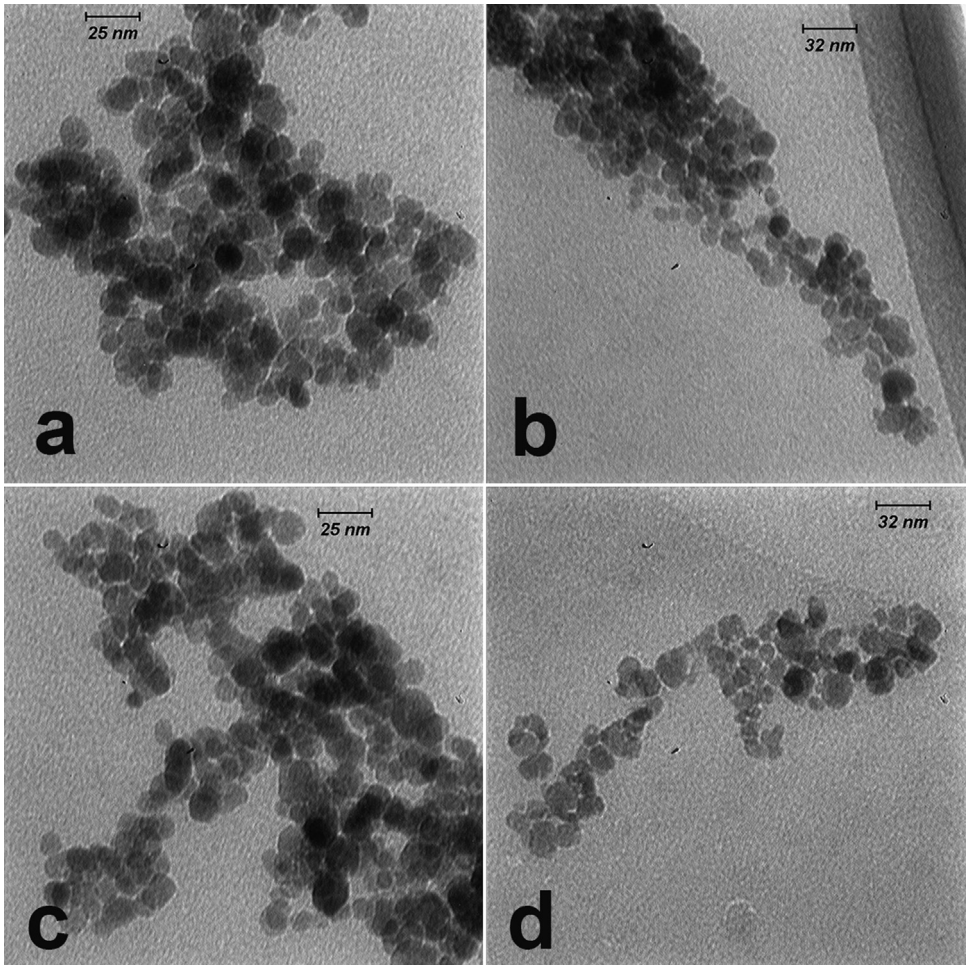


**Fig. 6.** The TEM micrographs of synthesized particles in presence of different chelating agents (Notations: (a) Citric sample, (b) Oxalic sample, (c) Stearic sample, and (d) Lauric sample).

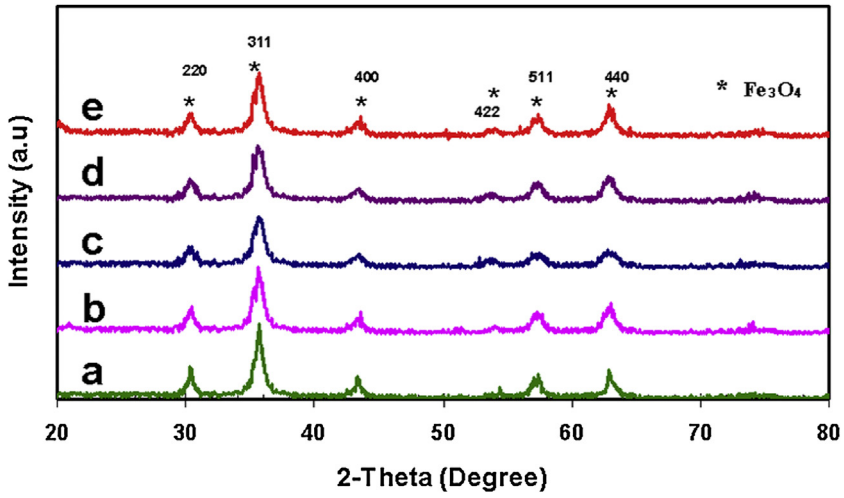


**Fig. 7.** The patterns of XRD analyses of different samples with and without chelating agents (Notations: (a) Pure $Fe_3O_4$, (b) Oxalic sample, (c) Lauric sample, (d) Stearic sample, and (e) Citric sample).

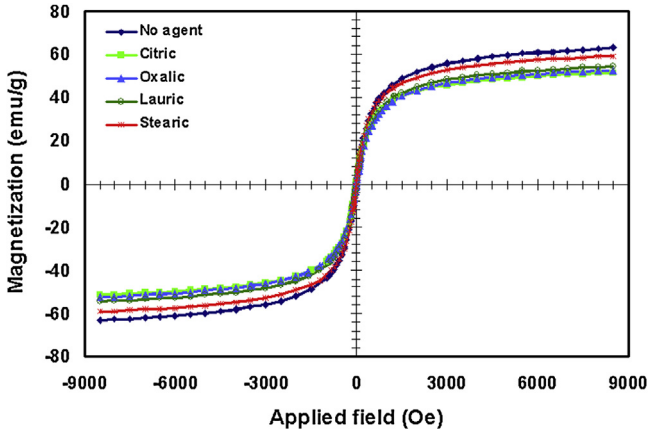


**Fig. 8.** The variation of magnetization amounts as a function of applied magnetic field for different samples (M-H curve).

This, again, emphasizes the negligible effect of chelating treatment on the structural properties of the synthesized nanoparticles.

## 4. Conclusions

The effects of different anionic chelating agents on the stability, structural, microstructural, and magnetic properties of synthesized $Fe_3O_4$ nanoparticles were investigated and the results are summarized as follows:

1 Based on DLS analyses, the hydrodynamic size of particles treated with 0.5, 1, 2 and 5 vol% of different chelating agents shows a minimum for 2 vol%.
2 According to zeta potential and FT-IR analyses, the zeta potential for oxalic and citric acids treated samples are more than the ones for stearic and lauric acids samples, which indicates their higher stabilization ability.
3 As results of DLS and TEM analyses, the particles size of oxalic and citric acid treated samples is lower while size distribution is considerably narrower than stearic and lauric acid treated nanoparticles, owing to their shorter chains.
4 Referring to XRD patterns, although the presence of chelating agents create no undesirable phases, their types can have effect on the peaks broadening. The peaks for oxalic and citric acid treated samples are sharper due to their lower particlesize (crystallites size).
5 XRD and VSM analyses indicate that the chelating agents and their types can negligibly affect the structural properties and magnetic behaviors of the synthesized nanoparticles.

## References

[1] Z.P. Xu, Q.H. Zeng, G.Q. Lu, A.B. Yu, Chem. Eng. Sci. 61 (3) (2006) 1027–1040.
[2] A.S. Lubbe, C. Bergemann, J. Brock, D.G. McClure, J. Magn. Magn. Mater. 194 (1–3) (1999) 149–155.
[3] H. Ai, C. Flask, B. Weinberg, X. Shuai, M.D. Pagel, D. Farrell, J. Duerk, J.M. Gao, Adv. Mater. 17 (16) (2005) 1949–1952.
[4] H. Lee, H.P. Shao, Y.Q. Huang, B. Kwak, IEEE Trans. Magn. 41 (10) (2005) 4102–4104.
[5] R. Jurgons, C. Seliger, A. Hilpert, L. Trahms, S. Odenbach, C. Alexiou, J. Phys.: Condens. Matter 18 (38) (2006) S2893–S2902.
[6] Y. Qiang, J. Antony, A. Sharma, J. Nutting, D. Sikes, D. Meyer, J. Nanopart. Res. 8 (3–4) (2006) 489–496.
[7] R.M. Cornell, U. Schwertmann, The Iron Oxides: Structure, Properties, Reactions Occurrences and Uses, second ed., Wiley-VCH, Weinheim, 2003.
[8] E. Murad, Series C: Mathematical and Physical Sciences, in: B.A. Stucki (Ed.), D. Reidel, 1985.
[9] U. Meisen, H. Kathrein, J. Imaging Sci. Technol. 44 (6) (2000) 508–513.
[10] R. Amini, M.R. Ghazanfari, M. Alizadeh, H. Ahmadi Ardakani, Structural, microstructural and thermal properties of lead-free bismuth–sodium–barium–titanate piezoceramics synthesized by mechanical alloying, Mater. Res. Bull. 48 (2013) 482–486.
[11] R. Amini, M.R. Ghazanfari, Effect of intermediate phases on the formation of nanostructured lead-free $(Bi_{0.5}\ Na_{0.5})_{0.94}\ Ba_{0.06}\ TiO_3$ piezoceramics by mechanical alloying, J. Alloys Compd. 587 (25) (2014) 520–526.
[12] H. Ahmadi Ardakani, M. Alizadeh, R. Amini, M.R. Ghazanfari, Dielectric properties of $CaCu_3Ti_4O_{12}$ improved by chromium/lanthanum co-doping, Ceram. Int. 38 (2012) 4217–4220.
[13] H. Ahmadi Ardakani, M. Alizadeh, R. Amini, M.R. Ghazanfari, M. Ghaffari, Structural and phase evolution in mechanically alloyed calcium copper titanate dielectrics, Ceram. Int. 39 (2013) 3307–3312.
[14] R.F. El-hajjar, S.S. Shams, D.J. Kehrl, Closed form solutions for predicting the elastic behavior of quasi-isotropic triaxially braided composites, Compos. Struct. 101 (2013) 1–8.
[15] M.R. Ghazanfari, R. Amini, S.F. Shams, M. Alizadeh, H. Ahmadi Ardakani, Effect of mechanical alloying synthesis process on the dielectric properties of $(Bi_{0.5}Na_{0.5})_{0.94}Ba_{0.06}TiO_3$ piezoceramics, Int. J. Mater. Res. Bull. 68 (2015) 260–266.
[16] S.S. Shams, R.F. ElHajjar, Investigation into the effects of fiber waviness in standard notched composite specimens, 6, CEAS Aeronaut. J. 4 (2015) 541–555.
[17] A.S. Teja, L.J. Holm, Supercritical Fluid Technology in Materials Science and Engineering: Synthesis, Properties, and Applications, in: Y.-P. Sun (Ed.), Elsevier, New York, 2002, pp. 327–349.
[18] A.S. Teja, P.Y. Koh, Synthesis, properties, and applications of magnetic iron oxide nanoparticles, Prog. Cryst. Growth Charact. Mater. 55 (1–2) (2009) 22–45.
[19] H. Yin, H.P. Too, G.M. Chow, The effects of particle size and surface coating on the cytotoxicity of nickel ferrite, Biomaterials 26 (29) (2005) 5818–5826.

[20] J. Lai, K.V.P.M. Shafi, A. Ulman, K. Loos, N.L. Yang, M.H. Cui, T. Vogt, C. Estournès, D.C. Locke, Mixed iron-manganese oxide nanoparticles, J. Phys. Chem. B 108 (39) (2004) 14876–14883.
[21] J.K. Oh, J.M. Park, Iron oxide-based superparamagnetic polymeric nanomaterials: design, preparation, and biomedical application, Prog. Polym. Sci. 36 (1) (2011) 168–189.
[22] D.S. Mathew, R.-S. Juang, An overview of the structure and magnetism of spinel ferrite nanoparticles and their synthesis in microemulsions, Chem. Eng. J. 129 (1–3) (2007) 51–65.
[23] D.S. Mathew, R.S. Juang, An overview of the structure and magnetism of spinel ferrite nanoparticles and their synthesis in microemulsions, Chem. Eng. J. 129 (1–3) (2007) 51–65.
[24] R.E. Rosensweig, Ferrofluids: Introduction, Encyclopedia of Materials: Science and Technology, in: K.H.J. Buschow, W.C. Robert, C.F. Merton, I. Bernard, J.K. Edward, M. Subhash, V. Patrick (Eds.), Elsevier, Oxford, 2001.
[25] A. LASCIALFARI, C. SANGREGORIO, Magnetic nanoparticles in biomedicine, Chim. Oggi Chem. Today 29 (2) (2011).
[26] B.D. Cullity, C.D. Graham, Introduction to Magnetic Materials, Wiley, New York, 2009.
[27] D.K. Kim, Y. Zhang, W. Voit, K.V. Rao, M. Muhammed, J. Magn. Magn. Mater. 225 (1–2) (2001) 30–36.
[28] A. Tavakoli, M. Sohrabi, A. Kargari, Chem. Pap. 61 (3) (2007) 151–170.
[29] Y.L. Hao, A.S. Teja, J. Mater. Res. 18 (2) (2003) 415–422.
[30] M. Ocana, R. Rodriguezclemente, C.J. Serna, Uniform colloidal particles in solution-formation mechanisms, Adv. Mater. 7 (1995) 212–216.
[31] J. Sun, S. Zhou, P. Hou, Y. Yang, J. Weng, X. Li, M. Li, Synthesis and characterization of biocompatible $Fe_3O_4$ nanoparticles, J. Biomed. Mater. Res. Part. A 10 (2006) 333–341.
[32] M. Mahdavi, M.B. Ahmad, M.J. Haron, M.Z. Ab Rahman, Optimized conditions for graft copolymerization of polyacrylamide onto rubberwood fibre, BioResources 6 (2011) 5110–5120.
[33] C.C. Hua, S. Zakaria, R. Farahiyan, L.T. Khong, K.L. Nguyen, M. Abdullah, S. Ahmad, Sizecontrolled synthesis and characterization of $Fe_3O_4$ nanoparticles by chemical coprecipitation method, Sains Malaysiana 37 (2008) 389–394.
[34] M. Mahdavi, M.B. Ahmad, M.J. Haron, Y. Gharayebi, K. Shameli, B. Nadi, Fabrication and characterization of $SiO_2$/(3-aminopropyl) triethoxysilane-coated magnetite nanoparticles for Lead(II) removal from aqueous solution, J. Inorg. Organomet. Polym. 23 (2013) 599–607.
[35] Y.F. Shen, J. Tang, Z.H. Nie, Y.D. Wang, Y. Ren, L. Zuo, Preparation and application of magnetic $Fe_3O_4$ nanoparticles for wastewater purification, Sep. Purif. Technol. 68 (2009) 312–319.
[36] M. Mahdavi, F. Namvar, M.B. Ahmad, R. Mohamad, Green biosynthesis and characterization of magnetic iron oxide ($Fe_3O_4$) nanoparticles using seaweed (Sargassum muticum) aqueous extract, Molecules 18 (2013) 5954–5964.
[37] F. Montagne, M.O. Monval, C. Pichot, H. Mozzanega, A. Elaissari, Preparation and characterization of narrow sized (O/w) magnetic emulsion, J. Magn. Magn. Mater. 250 (2002) 302–312.
[38] G.B. Deacon, R.J. Phillips, Relationship between the carbon–oxygenstretching frequencies of carboxylato complexes and the type of carboxylate coordination, Coord. Chem. Rev. 33 (1980) 227–250.
[39] N.L. Okassa, H. Marchais, L. Douziech-Eyrolles, K. Herve, S. Cohen-Jonathan, E. Munnier, M. Souce, C. Linassier, P. Dubois, I. Chourpa, Optimization of iron oxide nanoparticles encapsulation within poly(D,L-lactide-co-glycolide) sub-micron particles, Eur. J. Pharm. Biopharm. 67 (2007) 31–38.
[40] A.F. Thunemann, D. Schutt, L. Kaufner, U. Pison, H. Mohuald, Maghemite nanoparticles protectively coated with poly(ethylene imine) and poly(ethylene oxide)-blockpoly (glutamic acid), Langmuir 22 (2006) 2351–2357.
[41] J. Esquivel, I.A. Facundo, M.E. Trevino, R.G. Lopez, A novel method to prepare magnetic nanoparticles: precipitation in bicontinuous microemulsions, J. Mater. Sci. 42 (2007) 9015–9020.
[42] M. Mahdavi, M.B. Ahmad, M.J. Haron, F. Namvar, B. Nadi, M.Z. Ab Rahman, J. Amin, Synthesis, surface modification and characterisation of biocompatible magnetic iron oxide nanoparticles for biomedical applications, Molecules 18 (2013) 7533–7548.